Nonequilibrium master equation for interacting Brownian particles in a deep-well periodic potential

Michael W. Jack* and Adam Deaker
Department of Physics, University of Otago, P.O. Box 56, Dunedin 9054, New Zealand

(Received 4 March 2022; accepted 13 May 2022; published 31 May 2022)

Employing a creation and annihilation operator formulation, we derive an approximate many-body master equation describing discrete hopping from the more general continuous description of Brownian motion on a deep-well nonequilibrium periodic potential. The many-body master equation describes interactions of arbitrary strength and range arising from a "top-hat" two-body interaction potential. We show that this master equation reduces to the well-known asymmetric simple exclusion process and the zero range process in certain regimes. We also use the creation and annihilation operator formalism to derive results for the steady-state drift and the number fluctuations in special cases, including the unexplored limit of weak interparticle interactions.

DOI: 10.1103/PhysRevE.105.054150

I. INTRODUCTION

A wide range of out-of-equilibrium many-body systems can be described as interacting Brownian motion on a nonequilibrium time-independent periodic potential [1]. Examples include polymerization of nucleic acid [2–4], colloidal particles [5–8], and molecular motors [9,10]. When the potential is characterized by multiple deep wells, the continuous diffusion equation for the system can be approximated by a simpler discrete "master equation" describing thermally induced hopping between wells. Although this has been formally demonstrated for a single Brownian particle [11,12], there has been no systematic derivation for interacting particles—where a specific choice of interaction potential is required. In this paper we use a creation and annihilation formalism for identical nonquantum Brownian particles [13,14] to formally derive a discrete many-body master equation assuming a "top hat" two-body interaction potential. This derivation, based on well-defined and physically understandable approximations, provides physical insight into a number of well-known processes on discrete lattices that originally arose from either phenomenological [2] or mathematical consistency considerations [15].

A number of discrete equations have been used to describe the nonequilibrium dynamics of interacting entities (particles or molecules) experiencing thermally induced hopping on a discrete lattice [2,9,15–17]. These models have been shown to give rise to interesting collective behavior, including condensation into a collective mode [17] and "traffic jam"-like behavior [9]. The asymmetric simple exclusion process (ASEP) [2,15] is one of the simplest examples of a driven interacting system. It describes a system where interactions are strong enough to exclude two entities from occupying the same site (see Ref. [9] for a recent review). The zero range process (ZRP) [15] has been used to describe interactions between entities within the same site (see Ref. [16] for a recent review). Generalizations of these processes have also been considered [17]. The focus in much of this work has been either the application of these processes to describing particular experimental systems [3] or their mathematical solubility [17]. With a few exceptions [18,19], little attention has been paid to the derivation of these processes from a more general continuous Brownian motion theory or to determining under what conditions these processes are valid approximations. This is important as it can show which processes are physically possible and uncover deeper connections between processes normally regarded as separate. Creation and annihilation operator techniques provide a convenient method of carrying out this derivation.

In two seminal papers [13,14], Doi showed how to formulate many-body Brownian motion of identical *classical* particles using creation and annihilation operators. This modified quantum field theory (QFT) formalism can be shown to hold for classical particles in situations where neither phase coherence nor the uncertainty principle play a significant role [20]. This reformulation has subsequently been used in a number of areas of physics but has had the most application in the study of diffusion-limited chemical reactions [20], where diffusion usually occurs in an equilibrium potential. Similar to QFT, reformulating many-body Brownian motion in terms of creation and annihilation operators, enables a significant simplification through avoiding the need to track the coordinates of each individual particle and by succinctly incorporating the statistics (only bosonic in the Brownian case) of the identical particles [21]. This enables analysis to focus on the collective behavior of the system. It also enables many of the methods developed in analogous many-body quantum systems [21] to be directly available to the study of Brownian systems.

A creation and annihilation operator formalism could be very useful for describing interacting Brownian systems on nonequilibrium periodic potentials, however there has not yet been a systematic application of these methods to these systems. Operator methods have been utilized in isolated cases, including as a means of reformulating and solving the ASEP and ZRP [22,23]. In these cases, the operator formulation has

*michael.jack@otago.ac.nz

 ©2022 American Physical Society

been arrived at through mathematical arguments rather than through derivation from a more general continuous theory.

The main contribution of the current paper is a derivation of an approximate many-body master equation from a general continuous description with specific confining and interaction potentials. This derivation is based on a creation and annihilation operator formalism and an expansion in occupation-dependent localized states. The resulting master equation describes interactions with arbitrary strength and range arising from a top hat two-body interaction potential. In the case of an equilibrium potential and restricted range of interactions, the master equation reduces to that arrived at in Ref. [23] (see also Ref. [20]) from a less general starting point. In our derivation, all rates and interaction coefficients in the master equation can be related to the original potentials and all approximations are explicit, providing a clear physical interpretation of the resulting master equation and its regime of validity. We show how this master equation reduces to a number of well-known processes in various regimes and limits. A similar continuous system has been considered in Refs. [18,19] showing up to five different phases of behavior. However, Refs. [18,19] do not attempt a discrete description or use annihilation and creation operators and consider only hard-core interactions. As a second contribution, in this paper we demonstrate the use of creation and annihilation methods to solve the resulting master equation and explore the nonequilibrium steady state in a number of regimes, with a particular focus on the unexplored weak-interaction limit. We focus on studying how the steady-state drift and onsite number fluctuations are affected by the interactions in these regimes.

This paper is structured as follows. In Sec. II we review the general creation and annihilation operator formalism for indistinguishable Brownian particles. In Sec. III we use this general formalism to derive an approximate many-body master equation for noninteracting Brownian particles in a periodic potential. In Sec. IV we extend this to interacting particles by assuming a particular top-hat interaction potential. In this section we also show how this master equation can describe a number of well-known processes in various regimes and also present results for the drift and onsite number fluctuations in the nonequilibrium state. In Sec. V we conclude the paper and speculate on further applications of the creation and annihilation formalism in nonequilibrium Brownian systems.

II. CREATION OPERATOR FORMULATION OF MANY-BODY BROWNIAN MOTION

In this section we review the creation and annihilation formulation of many-body Brownian motion. This provides a background for readers unfamiliar with the approach, introduces our notation, and enables us to emphasize aspects of this formalism pertinent to later sections.

The probability density $P(x,t)$ of a single particle undergoing over-damped Brownian motion in a potential evolves via the Smoluchowski equation [24,25]:

$$\frac{\partial P(x,t)}{\partial t} = L_0(x)P(x,t), \tag{1}$$

where the single-particle evolution operator $L_0(x)$ is given by

$$L_0(x) = \frac{1}{\gamma}\frac{\partial}{\partial x}\left\{\left[\frac{\partial V_0(x)}{\partial x}\right] + k_B T\frac{\partial}{\partial x}\right\}, \tag{2}$$

and $V_0(x)$ is the single-particle potential. It is possible to make an eigenspectrum expansion of $L_0(x)$ similar to the Schrödenger equation [24,25].

Equation (1) can be written in a "bra" and "ket" form as

$$\frac{d|P(t)\rangle}{dt} = \hat{\mathcal{L}}|P(t)\rangle, \tag{3}$$

where $|P(t)\rangle$ is the state of the system and $\hat{\mathcal{L}}$ is the evolution operator, which is assumed to be time independent but not necessarily self adjoint. Note that $L_0(x)$ is only self adjoint if $V_0(x)$ is a confining potential.

The right and left eigenstates of $\hat{\mathcal{L}}$ are defined by

$$\hat{\mathcal{L}}|P_n\rangle = -\lambda_n|P_n\rangle, \tag{4}$$

$$\langle Q_n|\hat{\mathcal{L}} = -\lambda_n\langle Q_n|, \tag{5}$$

where the (in general) complex eigenvalues can be chosen such that $\mathrm{Re}\{\lambda_{n+1}\} > \mathrm{Re}\{\lambda_n\}$. One can show that the right and left eigenstates form a biorthonormal set:

$$\langle Q_m|P_n\rangle = \delta_{nm}, \tag{6}$$

$$\sum_n |P_n\rangle\langle Q_n| = \hat{\mathbb{1}}. \tag{7}$$

A physical description requires that we specify how averages of physical quantities are calculated. We confine our focus to the case where $\lambda_0 = 0$, such that a steady state $|P_{\mathrm{ss}}\rangle = |P_0\rangle$ (where $\hat{\mathcal{L}}|P_0\rangle = 0$) of the system exists. In this case, a self-consistent definition of the average of an operator $\hat{O}$ corresponding to a physical observable is given by

$$\langle O\rangle(t) \equiv \langle Q_0|\hat{O}|P(t)\rangle, \tag{8}$$

where $\langle Q_0|$ is the left eigenstate corresponding to $\lambda_0 = 0$. The normalization condition is given by

$$\langle Q_0|P(t)\rangle = 1, \tag{9}$$

which holds for all time (thus ensuring conservation of probability) $d\langle Q_0|P(t)\rangle/dt = \langle Q_0|\hat{\mathcal{L}}|P(t)\rangle = 0$ due to the fact that $\langle Q_0|\hat{\mathcal{L}} = 0$.

We can define a *preserving* transformation $|P'(t)\rangle = \hat{U}|P(t)\rangle$, with a well-defined inverse $\hat{U}^{-1}\hat{U} = \mathbb{1}$, such that it preserves Eq. (8):

$$\langle Q_0|\hat{O}|P(t)\rangle = \langle Q_0'|\hat{O}'|P'(t)\rangle, \tag{10}$$

where $\langle Q_0'| = \langle Q_0|\hat{U}^{-1}$ and $\hat{O}' = \hat{U}\hat{O}\hat{U}^{-1}$. For example, the time evolution operator $e^{\mathcal{L}t}$ is a preserving transformation which transfers the time dependence from the state $|P(t)\rangle$ to the operator $\hat{O}$ and gives rise to "Heisenberg" equations of motion:

$$\frac{d\hat{O}(t)}{dt} = [\hat{O}(t), \hat{\mathcal{L}}]. \tag{11}$$

It has been known for a long time that Fock-state methods or creation and annihilation operators can also be used for indistinguishable nonquantum particles or molecules [13,14].

Let us define creation and annihilation field operators $\hat{\psi}^\dagger(x)$ and $\hat{\psi}(x)$ via the following bosonic commutation relations:

$$[\hat{\psi}(x), \hat{\psi}^\dagger(x')] = \delta(x - x'), \tag{12}$$

$$[\hat{\psi}(x), \hat{\psi}(x')] = [\hat{\psi}^\dagger(x), \hat{\psi}^\dagger(x')] = 0. \tag{13}$$

We also use these to define the vacuum states $|\{0\}\rangle$ and $\langle\{0\}|$ by

$$\hat{\psi}(x)|\{0\}\rangle = 0, \quad \langle\{0\}|\hat{\psi}^\dagger(x) = 0. \tag{14}$$

Using these creation and annihilation operators, we can now formulate a dynamical description of a many-body classical system. To do this we assume that our evolution operator and state are functions of the creation and annihilation operators:

$$\hat{\mathcal{L}} = \hat{\mathcal{L}}[\hat{\psi}(x), \hat{\psi}^\dagger(x)], \tag{15}$$

$$|P(t)\rangle = f[\hat{\psi}^\dagger(x), t]|\{0\}\rangle. \tag{16}$$

With these definitions we can now straightforwardly apply the above "bra" and "ket" formulation of Eqs. (3)–(11) to describe a many-body system.

In the cases of interest here, the evolution operator conserves particle number, i.e., $[\hat{N}_{\rm tot}, \hat{\mathcal{L}}] = 0$, where $\hat{N}_{\rm tot} = \int dx \hat{\psi}^\dagger(x)\hat{\psi}(x)$. This means that $\langle Q_0| = \langle Q_0(N_{\rm tot})|$ has a definite number of particles $N_{\rm tot}$. In contrast, in Doi's original formulation [13] and many subsequent treatments [20] averages are defined in terms of a projection on a left-hand coherent state, which has Gaussian number fluctuations [28]. In this work we use the number-conserving definition given by Eq. (8). In the case when number is not conserved, or the exact number is not known, then to calculate averages it is a simple matter of calculating the weighted sum of $\langle Q_0(N_{\rm tot})|\hat{O}|P(t)\rangle$ over all numbers $N_{\rm tot}$ of interest.

III. MANY-BODY MASTER EQUATION FOR NONINTERACTING PARTICLES

Let us first consider noninteracting Brownian particles in a periodic potential. Over-damped Brownian motion of many noninteracting particles on a one-dimensional potential [11,26,27] can be described via the evolution operator

$$\hat{\mathcal{L}} = \int_{-\infty}^{\infty} dx \hat{\psi}^\dagger(x) L_0(x) \hat{\psi}(x), \tag{17}$$

where $L_0(x)$ is the single-particle evolution operator given by Eq. (2). This evolution operator conserves particle number as required. We assume that $V_0(x)$ is characterized by an out of equilibrium potential with multiple deep wells. As a concrete example, we consider a tilted periodic form,

$$V_0(x) = V_P(x) - fx, \tag{18}$$

where $V_P(x + L) = V_P(x)$. In addition, we assume that within a period L there are M potential wells with a characteristic spacing of $l = L/M$. The tilt $f \neq 0$ represents an external force driving the system out of equilibrium.

In the limit of deep potential wells, there is a timescale separation in the system whereby evolution within a well occurs much more rapidly than evolution between wells. In this limit, the description Eq. (17) can be transformed to a discrete master equation describing the long term behavior of thermally activated hopping between wells. A method of carrying this out formally has been presented in Ref. [12].

The method involves defining localized states in terms of fictional metastable potentials that match $V_0(x)$ at each minima and surrounding barriers [12] (more details are provided in Appendix A). The resulting states $\omega_n^m(x)$ and $\omega_n^{\dagger m}(x)$, where n denotes the well and m the mode of excitation, are localized about the nth well and form an over complete biorthonormal set. We can thus expand the operator of the full system as

$$\hat{\psi}(x) = \sum_{n,m} \hat{a}_n^m \omega_n^m(x), \tag{19}$$

$$\hat{\psi}^\dagger(x) = \sum_{n,m} \hat{a}_n^{\dagger m} \omega_n^{\dagger m}(x), \tag{20}$$

where $\hat{a}_n^{\dagger m}$ and $\hat{a}_n^m$ create and annihilate particles at the nth site in the mth mode. In the long-time limit of interest, for deep wells all higher modes $m > 0$ rapidly decay to the ground state and we can make the approximation

$$\hat{\psi}(x) \approx \sum_n \hat{a}_n \omega_n(x), \tag{21}$$

$$\hat{\psi}^\dagger(x) \approx \sum_n \hat{a}_n^\dagger \omega_n^\dagger(x), \tag{22}$$

where we have neglected higher ($m > 0$) modes and dropped the 0 superscript.

Inserting Eqs. (21) and (22) into Eq. (17) we can now write the evolution operator as

$$\hat{\mathcal{L}} = \sum_n \left[\kappa_n^- \hat{a}_{n-1}^\dagger \hat{a}_n + \kappa_n^+ \hat{a}_{n+1}^\dagger \hat{a}_n - (\kappa_n^- + \kappa_n^+)\hat{a}_n^\dagger \hat{a}_n\right], \tag{23}$$

where $\kappa_n^\pm$ are the hopping rates to neighboring sites. These rates are given by

$$\kappa_n^\pm = \int dx \omega_{n\pm1}^\dagger(x) L_0(x) \omega_n(x) \tag{24}$$

$$= -\int dx \omega_{n\pm1}^\dagger(x) \frac{\partial J(x)}{\partial x} \omega_n(x), \tag{25}$$

$$J(x) = \frac{k_b T}{\gamma} e^{-V_0(x)/k_B T} \frac{\partial}{\partial x} e^{V_0(x)/k_B T}, \tag{26}$$

where $L_0(x)$ has been written in terms of the current $J(x)$ in the second line. When $f \neq 0$ there is a difference between the forward and backward hopping rates $\kappa_n^+ \neq \kappa_n^-$ which pushes the system out of equilibrium.

A characteristic width of the localized state is provided by the curvature about the minima of the wells: $r_0 \sim \sqrt{k_b T / V''(x_n)}$. In the deep-well limit, $r_0 \ll l$, the hopping rates Eq. (24) reduce to the well-known Kramer's rates [24] (see Appendix A for more details). The Kramer's rates decrease exponentially with barrier height. Curvature about the well's minima and maxima also has an (albeit lesser) effect on the rates. In general, for a particular potential $V_0(x)$, it is necessary to numerically solve for the localized states and then use Eq. (24) to calculate the rates.

Equation (23) provides a natural generalization of the usual master equation description of a single Brownian particle [24] to the (noninteracting) many-body case. The first two terms describe hopping between adjacent wells and the last term

describes the escape process from each meta-stable well. The particular form of Eq. (23) ensures that a zeroth eigenvalue always exists and the system has a well-defined steady state.

The population at a single site is given by $\hat{n}_n = \hat{a}_n^\dagger \hat{a}_n$. From Eq. (11) we can derive an operator continuity equation of the form

$$\frac{d\hat{n}_n}{dt} = [\hat{n}_n, \hat{\mathcal{L}}] \tag{27}$$

$$= -(\hat{j}_n - \hat{j}_{n-1}), \tag{28}$$

where $\hat{j}_n = \kappa_n^+ \hat{a}_{n+1}^\dagger \hat{a}_n - \kappa_{n+1}^- \hat{a}_n^\dagger \hat{a}_{n+1}$ is the current operator.

Following previous work exploring the ASEP [9], for the M-well periodic system considered here [introduced earlier via Eq. (18)] we can write the full evolution operator as

$$\hat{\mathcal{L}} = \sum_{p=-\infty}^{\infty} \hat{\mathcal{L}}_p, \tag{29}$$

$$\hat{\mathcal{L}}_p = \sum_{n=1}^{M} \big[\kappa_n^- \hat{a}_{n-1,p}^\dagger \hat{a}_{n,p} + \kappa_n^+ \hat{a}_{n+1,p}^\dagger \hat{a}_{n,p} - (\kappa_n^- + \kappa_n^+) \hat{a}_{n,p}^\dagger \hat{a}_{n,p}\big], \tag{30}$$

where the p index denotes a set of M wells and $1 \leqslant n \leqslant M$, the position within the set. The wells are adjacent such that the operators satisfy $\hat{a}_{M+1,p} = \hat{a}_{1,p+1}$, $\hat{a}_{0,p} = \hat{a}_{M,p-1}$, $\hat{a}_{M+1,p}^\dagger = \hat{a}_{1,p+1}^\dagger$, and $\hat{a}_{0,p}^\dagger = \hat{a}_{M,p-1}^\dagger$.

The quantity of most interest in this system is the nonequilibrium steady-state drift per particle defined in terms of the average position:

$$v \equiv \frac{L}{N_{\text{tot}}} \frac{d\langle \hat{\mathcal{P}} \rangle(t)}{dt}\bigg|_{t\to\infty}, \tag{31}$$

where $\hat{\mathcal{P}} = \sum_{n=1}^{M} \sum_{p=-\infty}^{\infty} p \hat{n}_{n,p}$, $\hat{n}_{n,p} = \hat{a}_{n,p}^\dagger \hat{a}_{n,p}$ and the expectation value is determined by Eq. (8). From the Heisenberg equations of motion for $\hat{n}_{n,p}$, we determine

$$\frac{d\hat{\mathcal{P}}}{dt} = \sum_{n=1}^{M} \sum_{p=-\infty}^{\infty} \big[p\kappa_{n-1}^+ \hat{a}_{n,p}^\dagger \hat{a}_{n-1,p} - p\kappa_n^+ \hat{a}_{n+1,p}^\dagger \hat{a}_{n,p} + p\kappa_{n+1}^- \hat{a}_{n,p}^\dagger \hat{a}_{n+1,p} - p\kappa_n^- \hat{a}_{n-1,p}^\dagger \hat{a}_{n,p}\big] \tag{32}$$

$$= \sum_{n=1}^{M} \sum_{p=-\infty}^{\infty} \hat{j}_{n,p}, \tag{33}$$

where, in the first line, we have used the periodicity of the operators and also shifted the summation indices by 1. Defining the reduced operators by

$$\overline{\hat{o}_n} = \sum_{p=-\infty}^{\infty} \hat{o}_{n,p}, \tag{34}$$

we can write the drift as

$$v = \frac{L}{N_{\text{tot}}} \sum_{n=1}^{M} \langle \overline{\hat{j}_n} \rangle_{\text{ss}}. \tag{35}$$

We note that the reduced operators are periodic $\overline{\hat{o}_{n+M}} = \overline{\hat{o}_n}$ and their commutation relations are the same as for a single period. Suppose $[\hat{o}_{n,p}, \hat{o}'_{m,p}] = \hat{\Omega}_{n,m,p}$, then

$$[\overline{\hat{o}_n}, \overline{\hat{o}'_m}] = \sum_{p_1,p_2=-\infty}^{\infty} [\hat{o}_{n,p_1}, \hat{o}'_{m,p_2}]\delta_{p_1,p_2} \tag{36}$$

$$= \sum_{p_1=-\infty}^{\infty} \hat{\Omega}_{n,m,p_1} \tag{37}$$

$$= \overline{\hat{\Omega}_{n,m}}. \tag{38}$$

As $\hat{\mathcal{L}}$ in Eq. (29) can be written in terms of reduced operators, the Heisenberg equations for the reduced operators are the same as those for a single period. This means that the time evolution of a reduced operator can be determined by the equivalent operator on a single period by solving the evolution on that period. In other words, we can replace $\langle \overline{\hat{o}_n} \rangle(t)$ by $\langle \hat{o}_n \rangle(t)$, where $\langle \hat{o}_n \rangle(t)$ is found by solving the evolution determined by

$$\hat{\mathcal{L}}_R = \sum_{n=1}^{M} \big[\kappa_n^- \hat{a}_{n-1}^\dagger \hat{a}_n + \kappa_n^+ \hat{a}_{n+1}^\dagger \hat{a}_n - (\kappa_n^- + \kappa_n^+) \hat{a}_n^\dagger \hat{a}_n\big], \tag{39}$$

with the boundary conditions $\hat{a}_{M+1} = \hat{a}_1$, $\hat{a}_0 = \hat{a}_M$, $\hat{a}_{M+1}^\dagger = \hat{a}_1^\dagger$, and $\hat{a}_0^\dagger = \hat{a}_M^\dagger$. A similar argument has been made for calculating the drift on a periodic potential in the single-particle case [10].

The reduced evolution operator $\hat{\mathcal{L}}_R$ commutes with the number operator, $\hat{N} = \sum_{n=1}^{M} \hat{n}_n$, so the number of particles (denoted N) across the M sites is constant. For simplicity we take this to be an integer. As Eq. (39) is quadratic in annihilation and creation operators it can easily be diagonalized. In the special case of constant coupling constants $\kappa_n^\pm = \kappa_\pm$, the evolution operator Eq. (39) can be diagonalized as

$$\hat{\mathcal{L}}_R = -\sum_k \lambda_k \hat{c}_k^\dagger \hat{c}_k, \tag{40}$$

where we have introduced the new boson k-modes:

$$\hat{c}_k = \frac{1}{\sqrt{M}} \sum_{n=1}^{M} \hat{a}_n e^{-i2\pi kn/M}, \tag{41}$$

$$\hat{c}_k^\dagger = \frac{1}{\sqrt{M}} \sum_{n=1}^{M} \hat{a}_n^\dagger e^{i2\pi kn/M}. \tag{42}$$

The eigenvalues are given by [11]

$$\lambda_k = \kappa_+(1 - e^{-i2\pi k/M}) + \kappa_-(1 - e^{i2\pi k/M}). \tag{43}$$

This describes the eigenspectrum (in units of inverse time) of the $m = 0$ mode, or band, for $k = -(M-1)/2$ to $k = M/2$. The real part of λ_k gives the decay rate of the kth state. The master equation description is valid in the limit when the barrier heights for all sites are much greater than $k_B T$, and the gap to the $m = 1$ mode/band is large [12]. If $\kappa_+ \neq \kappa_-$, then the eigenspectrum gains an imaginary part representing overdamped oscillations and gives rise to a finite nonequilibrium steady-state drift. From Eq. (43) we see that $\lambda_0 = 0$ and thus the nonequilibrium steady state is given by the "condensation" of all N bosons into the zeroth mode $\hat{c}_0$: $|P_{\text{ss}}\rangle = |P_0\rangle = \frac{1}{\sqrt{N!}} \hat{c}_0^{\dagger N} |\{0\}\rangle$. This also tells us that the $\langle Q_0| = \frac{1}{\sqrt{N!}} \langle\{0\}| \hat{c}_0^N$.

Note that there is some freedom in the normalization of these states as long as $\langle Q_0|P_0\rangle = 1$.

Following the above discussion, the steady-state drift per particle is given by

$$v = \frac{L}{N}\sum_{n=1}^{M}\langle \hat{j}_n\rangle_{\rm ss}, \tag{44}$$

where we have normalized by N rather than $N_{\rm tot}$. Writing $\hat{j}_n$ in terms of the k modes we find

$$\hat{j}_n = \sum_k \hat{c}_k^\dagger \hat{c}_k\left(\kappa_+ e^{i2\pi k/M} - \kappa_- e^{-i2\pi k/M}\right). \tag{45}$$

Taking the expectation value in Eq. (44) gives

$$v = \frac{L}{N}\langle \hat{c}_0^\dagger \hat{c}_0\rangle_{\rm ss}(\kappa_+ - \kappa_-) \tag{46}$$

$$= v_0, \tag{47}$$

where $v_0 = L(\kappa_+ - \kappa_-)$ is the single-particle drift and we have used the fact that in the steady state all particles have condensed into the zeroth mode. Note that the many-body drift per particle is just the single-particle drift, as expected for a noninteracting system.

In a similar manner, we can also calculate the steady-state onsite number fluctuations:

$$\Delta n \equiv \langle \hat{n}_n^2\rangle_{\rm ss} - \langle \hat{n}_n\rangle_{\rm ss}^2 \tag{48}$$

$$= \langle \hat{a}_n^\dagger \hat{a}_n^\dagger \hat{a}_n \hat{a}_n\rangle_{\rm ss} + \langle \hat{n}_n\rangle - \langle \hat{n}_n\rangle_{\rm ss}^2. \tag{49}$$

Inserting the k modes given by Eqs. (41) and (42) we find

$$\Delta n = \frac{1}{M^2}\sum_{k_1,k_2,k_3,k_4}\langle \hat{c}_{k_1}^\dagger \hat{c}_{k_2}^\dagger \hat{c}_{k_3}\hat{c}_{k_4}\rangle_{\rm ss} e^{-i2\pi(k_1+k_2-k_3-k_4)/M}$$
$$+ \frac{1}{M}\sum_{k_1,k_2}\langle \hat{c}_{k_1}^\dagger \hat{c}_{k_2}\rangle_{\rm ss} e^{-i2\pi(k_1-k_2)/M}$$
$$- \frac{1}{M^2}\sum_{k_1,k_2,k_3,k_4}\langle \hat{c}_{k_1}^\dagger \hat{c}_{k_2}\rangle_{\rm ss}\langle \hat{c}_{k_3}^\dagger \hat{c}_{k_4}\rangle_{\rm ss} e^{-i2\pi(k_1-k_2+k_3-k_4)/M} \tag{50}$$

$$= \frac{1}{M^2}\langle \hat{c}_0^\dagger \hat{c}_0^\dagger \hat{c}_0 \hat{c}_0\rangle_{\rm ss} + \frac{1}{M}\langle \hat{c}_0^\dagger \hat{c}_0\rangle_{\rm ss} - \frac{1}{M^2}\langle \hat{c}_0^\dagger \hat{c}_0\rangle_{\rm ss}^2 \tag{51}$$

$$= \frac{N}{M}\left(1 - \frac{1}{M}\right), \tag{52}$$

where in the second and third lines we have again used the fact that in the steady-state limit, all the particles have condensed into the zeroth mode. For $M \gg 1$, $\Delta n \approx \rho$, where $\rho = N/M$, showing onsite number fluctuations similar to a coherent state [28].

IV. MANY-BODY MASTER EQUATION FOR INTERACTING PARTICLES

A many-body description becomes much more interesting once we consider interactions. When the presence of other particles alters the potential we can write

$$\hat{V}(x) = V_0(x)\hat{\mathbb{1}} + \int dx' \hat{\psi}^\dagger(x') V_I(x,x')\hat{\psi}(x'). \tag{53}$$

This additional contribution to the potential describes two-particle interactions and the evolution operator becomes

$$\hat{\mathcal{L}} = \int dx \hat{\psi}^\dagger(x) L_0(x)\hat{\psi}(x)$$
$$+ \frac{1}{\gamma}\int dx dx' \hat{\psi}^\dagger(x)\hat{\psi}^\dagger(x')\frac{\partial}{\partial x}\left[\frac{\partial V_I(x,x')}{\partial x}\right]\hat{\psi}(x)\hat{\psi}(x'). \tag{54}$$

Let us again assume a periodic potential $V_0(x)$ with a characteristic width between wells of l. Let us also assume that the particles have a certain interaction range, such that the interaction potential can be approximated by a "top-hat" potential of width $w \sim l$ about the particle position,

$$V_I(x,x') = \frac{\chi}{w}[\Theta(x - x' + w/2) - \Theta(x - x' - w/2)], \tag{55}$$

where χ is the interaction parameter with units of energy and $\chi > 0$ ($\chi < 0$) corresponds to repulsive (attractive) interactions, and $\Theta(x) = 0$ when $x < 0$ and $\Theta(x) = 1$ when $x > 0$. This potential describes particles with some finite extent that acts as a potential barrier to neighboring particles. For simplicity we assume that this range includes only neighboring sites, such that $w < 2l$. This restriction will be relaxed below.

Let us further assume, similar to the noninteracting case of Sec. III, that we are considering evolution in a tilted periodic potential where only the lowest band is occupied such that

$$\hat{\psi}(x) = \sum_{n,m}\hat{a}_n^m \tilde{\omega}_n^m(x), \tag{56}$$

$$\approx \sum_n \hat{a}_n \tilde{\omega}_n(x), \tag{57}$$

$$\hat{\psi}^\dagger(x) = \sum_{n,m}\hat{a}_n^{\dagger m}\tilde{\omega}_n^{\dagger m}(x), \tag{58}$$

$$\approx \sum_n \hat{a}_n^\dagger \tilde{\omega}_n^\dagger(x), \tag{59}$$

where in the second line we have neglected states with $m > 0$ and dropped the 0 superscript. As we will see below, the localized states $\tilde{\omega}_n(x)$ and $\tilde{\omega}_n^\dagger(x)$ are different from those in the noninteracting case.

Inserting this expansion into the interaction potential gives

$$\hat{V}(x) = V_0(x)\hat{\mathbb{1}} + \frac{\chi}{w}\sum_n \hat{n}_n \int_{x-w/2}^{x+w/2} dx' \tilde{\omega}_n^\dagger(x')\tilde{\omega}_n(x'). \tag{60}$$

Using the same arguments as in the noninteracting case we can derive an approximate evolution operator of the form

$$\hat{\mathcal{L}} = \sum_n\left[\hat{a}_{n-1}^\dagger \hat{\kappa}_n^- \hat{a}_n + \hat{a}_{n+1}^\dagger \hat{\kappa}_n^+ \hat{a}_n - \hat{a}_n^\dagger(\hat{\kappa}_n^- + \hat{\kappa}_n^+)\hat{a}_n\right], \tag{61}$$

where

$$\hat{\kappa}_n^\pm = -\int dx \tilde{\omega}_{n\pm1}^\dagger(x)\frac{\partial \hat{J}(x)}{\partial x}\tilde{\omega}_n(x), \tag{62}$$

$$\hat{J}(x) = \frac{k_b T}{\gamma} e^{-\hat{V}(x)/k_B T}\frac{\partial}{\partial x}e^{\hat{V}(x)/k_B T}, \tag{63}$$

and $\hat{V}(x)$ is given by Eq. (60).

From Eqs. (60) and (62) and the localized nature of the states $\tilde{\omega}_n(x)$ and $\tilde{\omega}_n^\dagger(x)$, it is clear that the rates only depend

on the number operators at sites in a finite region about site n and $n \pm 1$. Since we have restricted the range to $w < 2l$, the rates are only a function of the number operator at neighboring sites: $\hat{\kappa}_n^{\pm} = \hat{\kappa}_n^{\pm}(\hat{n}_n, \hat{n}_{n\pm1})$. We therefore need to evaluate the matrix elements

$$\kappa_n^{\pm}(N_n, N_{n\pm1}) = \langle N_n, N_{n\pm1}|\hat{\kappa}_n^{\pm}|N_n, N_{n\pm1}\rangle, \tag{64}$$

where $|\{N_n\}\rangle$ are the number states. These matrix elements can be calculated via Eq. (62) using the current operator

$$\kappa_n^{\pm}(N_n, N_{n\pm1}) = -\int dx \tilde{\omega}_{n\pm1}^{\dagger}(x) \frac{\partial J_{\{N_n\}}(x)}{\partial x} \tilde{\omega}_n(x), \tag{65}$$

$$J_{\{N_n\}}(x) = \frac{k_b T}{\gamma} e^{-V_{\{N_n\}}(x)/k_B T} \frac{\partial}{\partial x} e^{V_{\{N_n\}}(x)/k_B T}, \tag{66}$$

where

$$V_{\{N_n\}}(x) = V_0(x) + \frac{\chi}{w} \sum_{m=n,n\pm1} N_m \int_{x-w/2}^{x+w/2} dx' \tilde{\omega}_m^{\dagger}(x') \tilde{\omega}_m(x'). \tag{67}$$

Similar to the previous section, we define metastable potentials in terms of the effective many-body potential

$$\tilde{V}_n(x) = \begin{cases} V_{\{N_n\}}(x) & A_n < x < B_n, \\ -\infty & x = B_n \text{ and } x = A_n, \end{cases} \tag{68}$$

where $V_{\{N_n\}}(x)$ is given by Eq. (67). We use this to define localized states in terms of the eigenfunctions of this local metastable potential as follows:

$$\tilde{\omega}_n(x) = \begin{cases} \tilde{\psi}_n^0(x) & A_n \leqslant x \leqslant B_n, \\ 0 & x > B_n \text{ and } x < A_n, \end{cases} \tag{69}$$

$$\tilde{\omega}_n^{\dagger}(x) = \begin{cases} \tilde{\psi}_n^{\dagger 0}(x) & A_n \leqslant x \leqslant B_n, \\ 0 & x > B_n \text{ and } x < A_n, \end{cases} \tag{70}$$

where the eigenfunctions $\tilde{\psi}_n^m(x)$ and adjoints $\tilde{\psi}_n^{\dagger m}(x)$ of the nth metastable potential are given by

$$\tilde{\mathcal{L}}_n \tilde{\psi}_n^m(x) = -\tilde{\lambda}_n^m \tilde{\psi}_n^m(x), \tag{71}$$

$$\tilde{\mathcal{L}}_n^{\dagger} \tilde{\psi}_n^{\dagger m}(x) = -\tilde{\lambda}_n^m \tilde{\psi}_n^{\dagger m}(x), \tag{72}$$

where $\tilde{\mathcal{L}}_n$ and $\tilde{\mathcal{L}}_n^{\dagger}$ are, respectively, the evolution operator and its adjoint for the self-consistent metastable potential $\tilde{V}_n(x)$ on the nth well.

As the definition of the effective potential $V_{\{N_n\}}(x)$ contains the eigenfunctions $\tilde{\omega}_n(x)$, the system of equations Eqs. (67)–(72) needs to be solved self-consistently. We start with the noninteracting states and iterate until the eigenvalues reach a convergence tolerance.

A. Self-consistent localized states

The self-consistent approach can be illustrated by considering the change in the potential and states with occupation number. As an example system, we consider the noninteracting potential

$$V_0(x) = -\frac{A}{2} \cos(2\pi x/l), \tag{73}$$

with well minima at $x/l = -1, 0, 1$, which we label as site $n = 1,\ 2$, and 3, respectively.

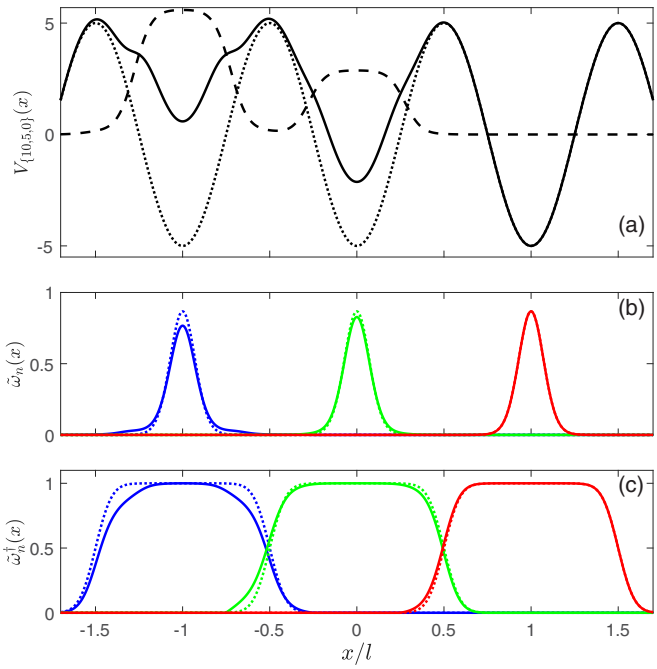

FIG. 1. Panel (a) shows the effective many-body potential $V_{\{N_n\}}(x)$ (solid line) for occupation numbers $\{N_n\} = \{10, 5, 0\}$. The noninteracting potential, V_0 [Eq. (73)] (dotted line), and interaction potential, V_I (dashed), are shown for comparison. Panel (b) shows the corresponding interacting localized states, $\tilde{\omega}_n(x)$ (solid), and noninteracting states (dotted). Panel (c) shows the adjoint interacting, $\tilde{\omega}_n^{\dagger}(x)$ (solid), and noninteracting (dotted) states. Parameters are $\chi = 2k_B T$ and $A = 10k_B T$ and $w = 0.55l$.

Consider the case where the wells have the occupation numbers $\{N_n\} = \{10, 5, 0\}$. Let us first consider the case where $w = 0.55l$ corresponding to an interaction that is largely contained within each well. The localized states and the many-body potential found using the self-consistent approach described above are shown in Fig. 1. Figure 1(a) shows how the occupation of the sites alters the potential to make the well on the left and middle shallower. This leads to a corresponding change in the localized states shown in Figs. 1(b) and 1(c).

We next consider the case where $w = 1.25l$, such that the interaction extends beyond a single potential well. Solving this system self-consistently, we find the effective potential and states shown in Fig. 2. In contrast to the $w = 0.55l$ case, the barriers have increased due to the overlap of the interacting potential. In this case, the localized states have not changed significantly from the noninteracting case.

The occupation of the states also has an important impact on the hopping rates. The rate of hopping $\kappa_n^{\pm}(N_n, N_{n\pm1})$ between the sites can be calculated from the interacting states $\tilde{\omega}_n(x)$ and $\tilde{\omega}_n^{\dagger}(x)$ via Eq. (65). In general this is a complicated function of the occupation numbers. In the deep-well limit this simplifies somewhat.

Let us consider the second term in the effective interaction potential Eq. (67) in the cases considered above (see Figs. 1 and 2). If $w < l$, then the effective interaction potential only has an onsite effect—decreasing the depth of the well with increasing occupation. This leads to an increase in hopping

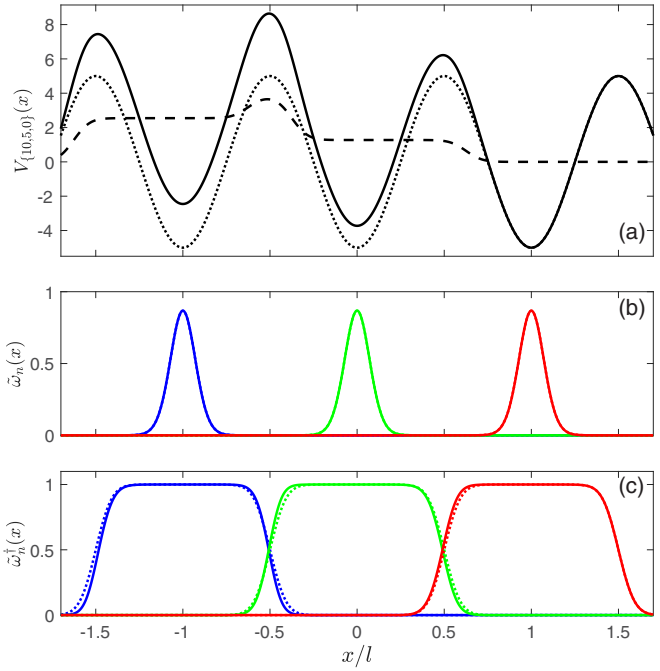

FIG. 2. Effective many-body potential (a), states (b), and adjoint states (c). Parameters are the same as in Fig. 1 but with $w = 1.25l$.

out of the well. In the deep-well limit $r_0 \ll w$, changes in curvature have a lesser effect [see Eqs. (A7) and (A9)]. If $2l > w > l$, then the interaction potential overlaps with the neighboring well—effectively increasing the barrier height between the wells as occupation increases (again with negligible change in curvature in the deep-well limit). This has a blocking effect on the hopping between wells. Finally, $w \approx l$ represents the intermediate case, where the well depth and the barrier height are both increased by a similar amount with occupation, and both blocking and increased hopping occur.

With these considerations, it is reasonable to assume the approximate functional form for the rates in the deep-well limit

$$\kappa_n^{\pm}(N_n, N_{n\pm1}) \approx \kappa_n^{\pm}(0,0)e^{-\beta_n N_{n\pm1}+\alpha_n N_n}. \tag{74}$$

A systematic numerical analysis of the rates confirms that Eq. (74) captures the key behavior. For example, in Fig. 3 we show the calculated hoping rates from the center site (site 2) to the left-most site (site 1), $\kappa_2^-(N_2, N_1)$, in the case $w = 0.55l$ for our three-site system varying the occupation at sites 1 and 2. For comparison, we have also plotted the functional form Eq. (74) with $\alpha_2 \approx \chi l/2\pi w k_b T$ and $\beta_2 \approx 0$. This shows excellent agreement to the numerical simulations. As another example, the hopping rate in the $w = 1.25l$ case is shown in Fig. 4. For comparison we have also plotted the functional form Eq. (74) with $\alpha_2 \approx 0$ and $\beta_2 \approx \chi l/2\pi w k_b T$. Finally, we consider the case where $w = l$. The hopping rates are shown in Fig. 5. The functional form Eq. (74) with $\alpha_2 \approx \beta_2 \approx \chi l/4\pi w k_b T$ is also provided for comparison.

B. Approximate master equation for interacting particles

Based on the functional from Eq. (74) found in the previous section, we conclude that one possible description of discrete

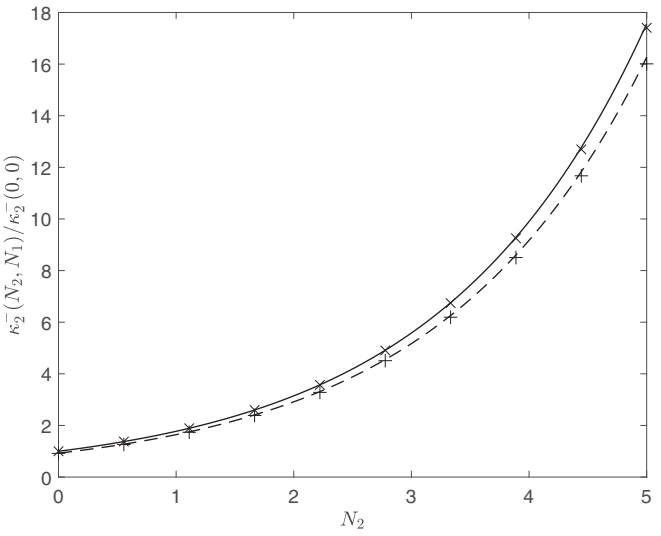

FIG. 3. Numerically calculated hopping rate $\kappa_2^-(N_2, N_1)$ as a function of N_2 for $N_1 = 0$ (+ symbols) and $N_1 = 10$ (× symbols) for $w = 0.55l$. The lines are fits for $N_1 = 0$ (solid) and $N_1 = 10$ (dotted) based on Eq. (74) with $\beta_2 = 0.008$ and $\alpha_2 = 0.573$. Other parameters are $A = 14k_bT$ and $\chi = 2k_bT$.

hopping in a periodic potential with interactions is via the evolution operator Eq. (61) with the hopping rates

$$\hat{\kappa}_n^{\pm} \approx \kappa_n^{\pm} e^{-\beta_n \hat{n}_{n\pm1}+\alpha_n \hat{n}_n}, \tag{75}$$

where $\alpha_n, \beta_n > 0$ are independent parameters reflecting the nature of the interaction. Equation (75) holds in the deep-well limit when the change in curvature of the wells and peaks is minimal and $r_0 \ll w < 2l$.

Confining ourselves to the limit where $r_0 \ll w$, it is straightforward to generalize the above to a top-hat potential with long range ($w \gg l$) or attractive ($\chi < 0$) interactions.

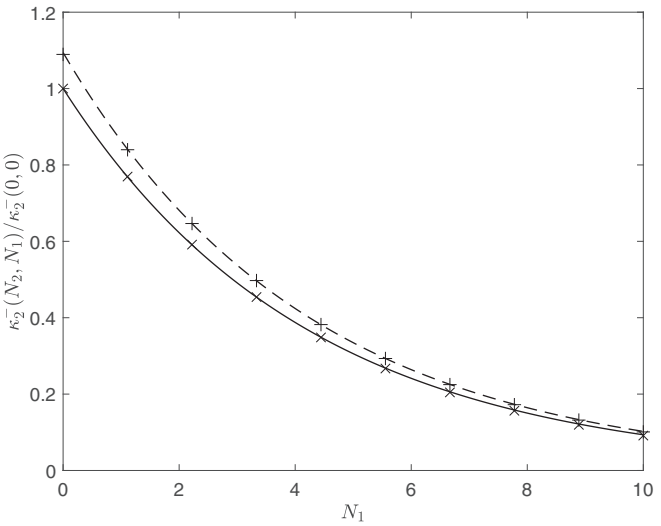

FIG. 4. Numerically calculated hopping rate $\kappa_2^-(N_2, N_1)$ as a function of N_1 for $N_2 = 0$ (+ symbols) and $N_2 = 5$ (× symbols) for $w = 1.25l$. The lines are fits for $N_2 = 0$ (solid) and $N_2 = 5$ (dotted) based on Eq. (74) with $\beta_2 = 0.237$ and $\alpha_2 = 0.018$. Other parameters are $A = 14k_bT$ and $\chi = 2k_bT$.

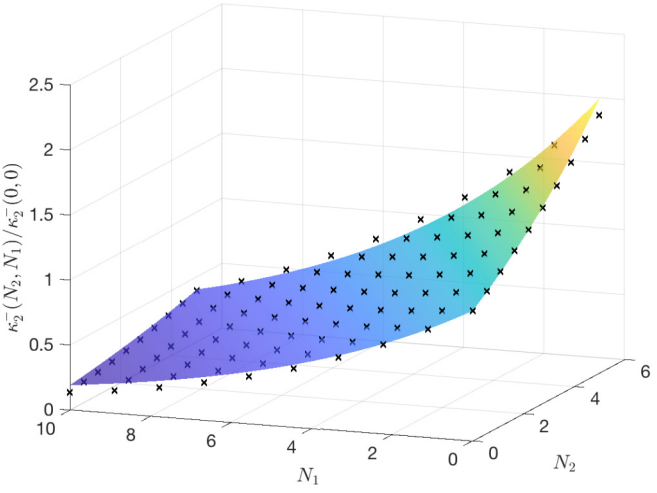

FIG. 5. Numerically calculated hopping rate $\kappa_2^-(N_2, N_1)$ as a function of N_1 and N_2 ($\times$ symbols) for $w = 1.0l$. The surface is a fit based on Eq. (74) with $\beta_2 = 0.165$ and $\alpha_2 = 0.149$. Other parameters are $A = 14k_bT$ and $\chi = 2k_bT$.

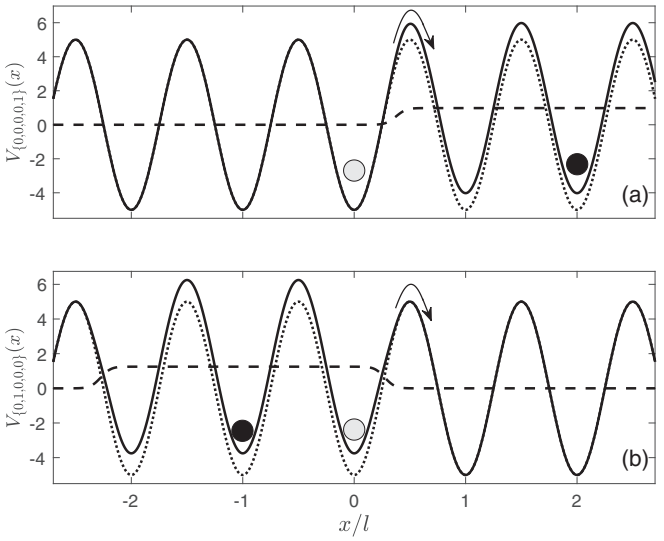

FIG. 6. The effective many-body potential $V_{\{N_n\}}(x)$, (solid line) experienced by a particle (centre grey dot) due to the presence of another particle (black dot) at $d = 2$ sites away. The noninteracting potential, V_0 [Eq. (73)] (dotted line), and interaction potential, V_I (dashed), are shown for comparison. In (a) $\{N_n\} = \{0, 0, 0, 0, 1\}$, and the interaction width is $w = 3.25l$. In (b) $\{N_n\} = \{0, 1, 0, 0, 0\}$, and the interaction width is $w = 2.55l$. A forward hop from the center well (gray dot) in case (a) will experience a higher barrier and in case (b) a lower barrier due to the interaction. Parameters are $A = 10k_bT$ and $\chi = 20k_bT$.

Following the pattern of behavior seen in the previous section for the top hat potential, a hopping transition to a neighboring well will be affected by population in the other wells in two distinct ways. Either population in sites an interaction width in the forward direction will *increase* the barrier height or, population an interaction width in the reverse direction will have raised the well minimum height (resulting in a *decrease* in the forward barrier height). These two possibilities are illustrated in Fig. 6. Thus, for interactions of arbitrary width, w, the coupling rate can be written

$$\hat{\kappa}_n^{\pm} \approx \kappa_n^{\pm} e^{-\beta_n \hat{n}_{n\pm d} + \alpha_n \hat{n}_{n\mp(d-1)}}, \tag{76}$$

where $d \geqslant 1$, such that the forward (backward) hopping rate to the neighboring site depends on the population d sites away in the forward (backward) direction and $d - 1$ in the backward (forward) direction. In the uniform-spaced-well case $d = \lceil w/2l \rceil$. In addition, for the attractive case when $\chi < 0$, the effect of the interaction on the potential is reversed, such that Eq. (76) can also encompass the attractive case with $\alpha_n, \beta_n < 0$ [1]. The general effective many-body evolution operator for a top-hat potential is therefore given by

$$\begin{aligned}\hat{\mathcal{L}} = \sum_n \big[&\kappa_n^+ \hat{a}_{n+1}^\dagger e^{-\beta_n \hat{n}_{n+d} + \alpha_n \hat{n}_{n-(d-1)}} \hat{a}_n \\ &+ \kappa_n^- \hat{a}_{n-1}^\dagger e^{-\beta_n \hat{n}_{n-d} + \alpha_n \hat{n}_{n+(d-1)}} \hat{a}_n \\ &- \kappa_n^+ \hat{a}_n^\dagger e^{-\beta_n \hat{n}_{n+d} + \alpha_n \hat{n}_{n-(d-1)}} \hat{a}_n \\ &- \kappa_n^- \hat{a}_n^\dagger e^{-\beta_n \hat{n}_{n-d} + \alpha_n \hat{n}_{n+(d-1)}} \hat{a}_n \big].\end{aligned} \tag{77}$$

The first two terms describe hopping between adjacent sites with a hopping rate that is modified by the occupation in sites d and $d - 1$ sites away. The last two terms account for the decay of each meta-stable well and also depends on the occupation in the same sites. As in the noninteracting case, the particular form ensures that a zeroth eigenvalue always exists and the system has a well-defined steady state. The continuity equation in this case becomes

$$\frac{d\hat{n}_n}{dt} = -(\hat{j}_n - \hat{j}_{n-1}), \tag{78}$$

$$\begin{aligned}\hat{j}_n = &\kappa_n^+ \hat{a}_{n+1}^\dagger e^{-\beta_n \hat{n}_{n+d} + \alpha_n \hat{n}_{n-(d-1)}} \hat{a}_n \\ &- \kappa_{n+1}^- \hat{a}_n^\dagger e^{-\beta_{n+1} \hat{n}_{n-d+1} + \alpha_{n+1} \hat{n}_{n+d}} \hat{a}_{n+1},\end{aligned} \tag{79}$$

where $\hat{j}_n$ is the current operator.

The master equation defined by the evolution operator Eq. (77) describes discrete hopping between next-neighbor wells and interactions of arbitrary strength and range due to a top hat potential. This is the main result of this paper. Note that we have only considered the simplest case of a top-hat potential, more general potentials will lead to more complex types of number dependence in the hopping rates. For simplicity, in the remainder of this paper we consider only the cases where $d = 1$ and $\alpha_n, \beta_n > 0$.

A master equation of the form Eq. (77) has been presented previously in Ref. [23], however their treatment did not provide a derivation from a specific confining or interaction potential.

For an M-periodic system, as discussed in the noninteracting case, we can again show that expectation values of reduced operators can be determined by solving a reduced

system evolution operator

$$\hat{\mathcal{L}}_R = \sum_{n=1}^{M} \big[\kappa_n^+ \hat{a}_{n+1}^\dagger e^{-\beta_n \hat{n}_{n+1} + \alpha_n \hat{n}_n} \hat{a}_n + \kappa_n^- \hat{a}_{n-1}^\dagger e^{-\beta_n \hat{n}_{n-1} + \alpha_n \hat{n}_n} \hat{a}_n - \hat{a}_n^\dagger (\kappa_n^- e^{-\beta_{n-1} \hat{n}_{n-1} + \alpha_n \hat{n}_n} + \kappa_n^+ e^{-\beta_n \hat{n}_{n+1} + \alpha \hat{n}_n}) \hat{a}_n \big]. \tag{80}$$

In particular, the drift is given by Eq. (44) for the reduced system defined by Eq. (80). A systematic exploration of this system is left for future work. Instead, here we consider three particular limiting regimes.

C. Zero range process

If $\beta_n = 0$ for all sites, then there are only onsite interactions. In this case the master equation reduces to

$$\hat{\mathcal{L}} = \sum_n \big[\kappa_n^+ \hat{a}_{n+1}^\dagger e^{\alpha_n \hat{n}_n} \hat{a}_n + \kappa_n^- \hat{a}_{n-1}^\dagger e^{\alpha_n \hat{n}_n} \hat{a}_n - \hat{a}_n^\dagger (\kappa_n^- e^{\alpha_n \hat{n}_n} + \kappa_n^+ e^{\alpha \hat{n}_n}) \hat{a}_n \big]. \tag{81}$$

We can recognize Eq. (81) as the operator form of the ZRP [22,23]. From the above derivation, the ZRP can be interpreted as the case where the range of the interactions is less than the width of each cell. More precisely, the ZRP holds in the regime where $r_0 \ll w < l$. In other words the ZRP holds in the regime where the curvature of the wells are not altered by the interaction (see discussion at end of Sec. IV A). In this sense it is not really "zero range." The cases where $r_0 \sim w$ or $r_0 \gg w$ are left for future work.

Confining ourselves to the homogeneous case ($\kappa_\pm = \kappa_n^\pm$), we can write the reduced evolution operator as

$$\hat{\mathcal{L}}_R = \sum_{n=1}^{M} \big[\kappa_+ (\hat{a}_{n+1}^\dagger - \hat{a}_n^\dagger) \hat{A}_n + \kappa_- (\hat{a}_{n-1}^\dagger - \hat{a}_n^\dagger) \hat{A}_n \big], \tag{82}$$

where we have defined the operator $\hat{A}_n = e^{\alpha \hat{n}_n} \hat{a}_n$. We can also define the adjoint operator by $\hat{A}_n^\dagger = e^{-\alpha(\hat{n}_n - 1)} \hat{a}_n^\dagger$ such that they satisfy the boson commutation relations $[\hat{A}_n, \hat{A}_m^\dagger] = \delta_{n,m}$.

Introducing the k-mode operators

$$\hat{C}_k = \frac{1}{\sqrt{M}} \sum_{n=1}^{M} \hat{A}_n e^{-i2\pi kn/M}, \tag{83}$$

$$\hat{C}_k^\dagger = \frac{1}{\sqrt{M}} \sum_{n=1}^{M} \hat{A}_n^\dagger e^{i2\pi kn/M}, \tag{84}$$

which also satisfy boson commutation relations, we can write the evolution operator Eq. (82) as

$$\hat{\mathcal{L}}_R = -\sum_k \lambda_k \hat{c}_k^\dagger \hat{C}_k, \tag{85}$$

where λ_k is given by Eq. (43) and $\hat{c}_k^\dagger$ by Eq. (42).

This form of the evolution operator suggests that $\langle Q_0| \propto \langle\{0\}|c_0^N$ as in the noninteracting case. The bosonic nature of $\hat{C}_k$ tells us that in the steady state all particles have condensed into a single boson mode: $|P_{\rm ss}\rangle \propto \hat{C}_0^{\dagger N}|\{0\}\rangle$. This boson mode $\hat{C}_0$ is very different from the noninteracting case when $\alpha \neq 0$. Due to the nontrivial commutation relations between $\hat{c}_k$ and $\hat{C}_k^\dagger$, it is not straight forward to derive analytical expressions for the drift and number fluctuations for this case so we leave their calculation for later work.

D. ASEP limit

In the case where $l < w < 2l$, the range of interaction is such that $\beta_n \gg \alpha_n$ and the effect of α_n can be neglected. Let us also assume strong interparticle interactions such that that $\beta_n \gg 1$. We can understand this limit by considering the effect of the hopping term $\hat{a}_{n+1}^\dagger e^{-\beta_n \hat{n}_{n+1}} \hat{a}_n$ on a simple two site system:

$$\hat{a}_2^\dagger e^{-\beta_1 \hat{n}_2} \hat{a}_1 |1,0\rangle = |0,1\rangle, \tag{86}$$

$$\hat{a}_2^\dagger e^{-\beta_1 \hat{n}_2} \hat{a}_1 |2,0\rangle = \sqrt{2}|1,1\rangle, \tag{87}$$

$$\hat{a}_2^\dagger e^{-\beta_1 \hat{n}_2} \hat{a}_1 |1,1\rangle = \sqrt{2} e^{-\beta_1} |0,2\rangle, \tag{88}$$

$$\hat{a}_2^\dagger e^{-\beta_1 \hat{n}_2} \hat{a}_1 |2,1\rangle = 2e^{-\beta_1} |1,2\rangle. \tag{89}$$

From this, it is clear that if $\beta_1 \gg 1$ then the transition $|2,0\rangle \to |1,1\rangle$ will be much more likely than the inverse. This means that interactions will cause more rapid diffusion to a uniform distribution across the sites and onsite number fluctuations will be small. It also means that a particle is unlikely to jump to a site that is already occupied. In the case when there are on average less than one particle per site, we can then make the approximation

$$\hat{a}_n \approx \hat{\sigma}_n, \tag{90}$$

$$\hat{a}_n^\dagger \approx \hat{\sigma}_n^\dagger, \tag{91}$$

$$\hat{a}_{m'}^\dagger e^{-\beta_m \hat{n}_{m'}} \hat{a}_m \approx \hat{\sigma}_{m'}^\dagger \hat{\sigma}_m, \tag{92}$$

$$\hat{a}_m^\dagger e^{-\beta_m \hat{n}_{m'}} \hat{a}_m \approx \hat{\sigma}_m^\dagger \hat{\sigma}_{m'}^\dagger \hat{\sigma}_{m'} \hat{\sigma}_m, \tag{93}$$

for $m' \neq m$, where $\hat{\sigma}_m$ and $\hat{\sigma}_m^\dagger$ are the Pauli matrices, satisfying $[\hat{\sigma}_n^z, \hat{\sigma}_m] = -2\hat{\sigma}_n \delta_{nm}$, $[\hat{\sigma}_n^z, \hat{\sigma}_m^\dagger] = 2\hat{\sigma}_n^\dagger \delta_{nm}$ and $[\hat{\sigma}_n^\dagger, \hat{\sigma}_m] = \hat{\sigma}_n^z \delta_{nm}$. As $\hat{\sigma}_m^{\dagger 2} = \hat{\sigma}_m^2 = 0$ two particles cannot occupy a single site.

In this limit, we can write the effective evolution and current as

$$\hat{\mathcal{L}} = \sum_n \big[\kappa_n^- \hat{\sigma}_{n-1}^+ \hat{\sigma}_n + \kappa_n^+ \hat{\sigma}_{n+1}^\dagger \hat{\sigma}_n - (\kappa_n^- \hat{\sigma}_{n-1}^\dagger \hat{\sigma}_{n-1} + \kappa_n^+ \hat{\sigma}_{n+1}^\dagger \hat{\sigma}_{n+1}) \hat{\sigma}_n^\dagger \hat{\sigma}_n \big], \tag{94}$$

$$\hat{j}_n = \kappa_n^+ \hat{\sigma}_{n+1}^\dagger \hat{\sigma}_n - \kappa_{n+1}^- \hat{\sigma}_n^+ \hat{\sigma}_{n+1}. \tag{95}$$

Equation (94) is the operator form of the ASEP [9,29]. The ASEP can therefore be interpreted as the case where strong repulsive interactions exclude multiple occupation of each site.

To calculate the steady, state drift we follow the same argument as before and consider only the reduced system

$$\hat{\mathcal{L}}_R = \sum_{n=1}^{M} \big[\kappa_n^- \hat{\sigma}_{n-1}^+ \hat{\sigma}_n + \kappa_n^+ \hat{\sigma}_{n+1}^\dagger \hat{\sigma}_n - (\kappa_n^- \hat{\sigma}_{n-1}^\dagger \hat{\sigma}_{n-1} + \kappa_n^+ \hat{\sigma}_{n+1}^\dagger \hat{\sigma}_{n+1}) \hat{\sigma}_n^\dagger \hat{\sigma}_n \big]. \tag{96}$$

The drift requires calculation of $\langle\hat{\sigma}^{\dagger}_{n+1}\hat{\sigma}_n\rangle_{\rm ss} = \langle\hat{\sigma}^{\dagger}_n\hat{\sigma}_{n+1}\rangle_{\rm ss}$. These can be calculated in various ways. An operator approach (see Appendix B) gives $\langle\hat{\sigma}^{\dagger}_{n+1}\hat{\sigma}_n\rangle_{\rm ss} = N(M-N)/M(M-1)$, such that

$$v = v_0\frac{1-\rho}{1-1/M}. \tag{97}$$

The steady-state onsite number fluctuations (see Appendix B) are

$$\Delta n = \langle(\hat{\sigma}^{\dagger}_n\hat{\sigma}_n)^2\rangle_{\rm ss} - \langle\hat{\sigma}^{\dagger}_n\hat{\sigma}_n\rangle^2_{\rm ss} \tag{98}$$

$$= \langle\hat{\sigma}^{\dagger}_n\hat{\sigma}_n\rangle_{\rm ss}(1-\langle\hat{\sigma}^{\dagger}_n\hat{\sigma}_n\rangle_{\rm ss}) \tag{99}$$

$$= \rho(1-\rho). \tag{100}$$

Equations (97) and (100) show the characteristic blocking of the hopping in the ASEP as $\rho \to 1$.

More generally, Eq. (96) can be mapped to a quantum Hamiltonian of a spin-1/2 ferromagnet [30,31]. This is an integrable model and can be solved by the Bethe ansatz. Thus, writing the ASEP process in this operator form allows the application of well-developed mathematical techniques from quantum mechanics.

We conclude from this section that the evolution operator Eq. (77), provides a description of many-body hopping from the noninteracting ($\alpha_n = \beta_n = 0$) to the strong-interacting ASEP limit.

E. Weakly interacting system

In this section we consider the limit of a weakly interacting system. In this limit, the coupling constant Eq. (75) can be expanded to first order in β_n and α_n as

$$\hat{\kappa}^{\pm}_n \approx \kappa^{\pm}_n(1-\beta_n\hat{n}_{n\pm1}+\alpha_n\hat{n}_n). \tag{101}$$

Considering a M-periodic system as before and dropping the n dependence on the hopping rates and interaction coefficients the evolution operator Eq. (80) and current become

$$\hat{\mathcal{L}}_R = \sum_{n=1}^{M}\big[\kappa_-(\hat{a}^{\dagger}_{n-1}-\hat{a}^{\dagger}_n)(1-\beta\hat{n}_{n-1}+\alpha\hat{n}_n)\hat{a}_n + \kappa_+(\hat{a}^{\dagger}_n-\hat{a}^{\dagger}_n)(1-\beta\hat{n}_{n+1}+\alpha\hat{n}_n)\hat{a}_n\big], \tag{102}$$

$$\hat{j}_n = \kappa_+\hat{a}^{\dagger}_{n+1}(1-\beta\hat{n}_{n+1}+\alpha\hat{n}_n)\hat{a}_n - \kappa_-\hat{a}^{\dagger}_n(1-\beta\hat{n}_n+\alpha\hat{n}_{n+1})\hat{a}_{n+1}. \tag{103}$$

In the analogous quantum system—the Bose-Hubbard model—the weakly interacting limit is treated using the Bogoliubov method [32]. We can use a similar approach for the current system. In this method we assume a macroscopic number of particles across the $M \gg 1$ sites and also that the interactions are weak such that most of the N particles in the system are condensed into the ground state mode $\hat{c}_0$. In this limit, we can replace the ground state operators by complex numbers: $\hat{c}_0 = \hat{c}^{\dagger}_0 \to \sqrt{N}$. Transforming to the noninteracting k mode Eqs. (41) and (42) and neglecting terms smaller than N in Eq. (102) we arrive at the approximate evolution operator

$$\hat{\mathcal{L}}_R \approx \sum_k\left[-\Lambda_k\hat{c}^{\dagger}_k\hat{c}_k + \frac{1}{2}\mu_k\hat{c}^{\dagger}_k\hat{c}^{\dagger}_{-k}\right], \tag{104}$$

where

$$\Lambda_k = 2\rho[\alpha\lambda_k - \beta(\kappa_+-\kappa_-)i\sin(2\pi k/M)] + \lambda_k, \tag{105}$$

$$\mu_k = -2\rho(\kappa_++\kappa_-)(\alpha+\beta)[1-\cos(2\pi k/M)]. \tag{106}$$

In the usual Bogoliubov treatment this evolution operator is diagonalized via a linear transformation [32]. This is also possible here. Defining new boson modes by

$$\hat{b}_k = \hat{c}_k - \hat{c}^{\dagger}_{-k}\frac{\mu_k}{\Lambda_k+\Lambda_{-k}}, \tag{107}$$

$$\hat{b}^{\dagger}_k = \hat{c}^{\dagger}_k, \tag{108}$$

and the inverse

$$\hat{c}_k = \hat{b}_k + \hat{b}^{\dagger}_{-k}\frac{\mu_k}{\Lambda_k+\Lambda_{-k}}, \tag{109}$$

$$\hat{c}^{\dagger}_k = \hat{b}^{\dagger}_k, \tag{110}$$

we can write the evolution operator in the diagonal form

$$\hat{\mathcal{L}}_R = -\sum_k \Lambda_k\hat{b}^{\dagger}_k\hat{b}_k. \tag{111}$$

Note that although the mode operators $\hat{b}_k$ and $\hat{b}^{\dagger}_k$ satisfy boson commutation relations, they are not related by an adjoint operation.

The spectrum, Λ_k, of the boson excitations is modified by the interactions. The decay of the excited modes, given by the real part of Λ_k, becomes

$$\mathrm{Re}\{\Lambda_k\} = (1+2\rho\alpha)\mathrm{Re}\{\lambda_k\} \tag{112}$$

$$= 2(1+2\rho\alpha)(\kappa_++\kappa_-)[1-\cos(2\pi k/M)]. \tag{113}$$

Showing that the decay of the excitations is independent of β. The imaginary part of the spectrum is given by

$$\mathrm{Im}\{\Lambda_k\} = [1+2\rho(\alpha-\beta)]\mathrm{Im}\{\lambda_k\} \tag{114}$$

$$= 2[1+2\rho(\alpha-\beta)](\kappa_+-\kappa_-)\sin(2\pi k/M). \tag{115}$$

Showing that, in the Bogoliubov limit, the noninteracting oscillations are only modified if $\alpha \neq \beta$. The excitation spectrum is shown in Fig. 7.

Since $\Lambda_0 = 0$, as in the noninteracting case, the nonequilibrium steady state is characterized by all the particles condensing into the zeroth mode $\hat{c}_0 = \hat{b}_0$, $\hat{c}^{\dagger}_0 = \hat{b}^{\dagger}_0$ such that $\langle Q_0|\hat{b}^{\dagger}_k = \sqrt{N}\delta_{k,0}\langle Q_0|$ and $\hat{b}_k|P(0)\rangle = |P(0)\rangle\sqrt{N}\delta_{k,0}$. To calculate the drift we require the expectation value of the current operator [see Eq. (44)]. Writing the current operator Eq. (103) in terms of the k modes we find

$$\hat{j}_n = \sum_{k_1}\hat{c}^{\dagger}_{k_1}\hat{c}_{k_1}\Delta K_{k_1} + \frac{1}{M}\sum_{k_1,k_2,k_3}\hat{c}^{\dagger}_{k_1}\hat{c}^{\dagger}_{k_2}\hat{c}_{k_3}\hat{c}_{k_3-k_1-k_2}\Delta G_{k_1,k_2-k_3}, \tag{116}$$

where $\Delta K_k = (\kappa_+e^{-i2\pi k/M} - \kappa_-e^{i2\pi k/M})$ and

$$\Delta G_{k,k'} = \kappa_+e^{-i2\pi k/M}(\alpha-\beta e^{-i2\pi k'/M}) - \kappa_-e^{i2\pi k/M}(\alpha-\beta e^{i2\pi k'/M}). \tag{117}$$

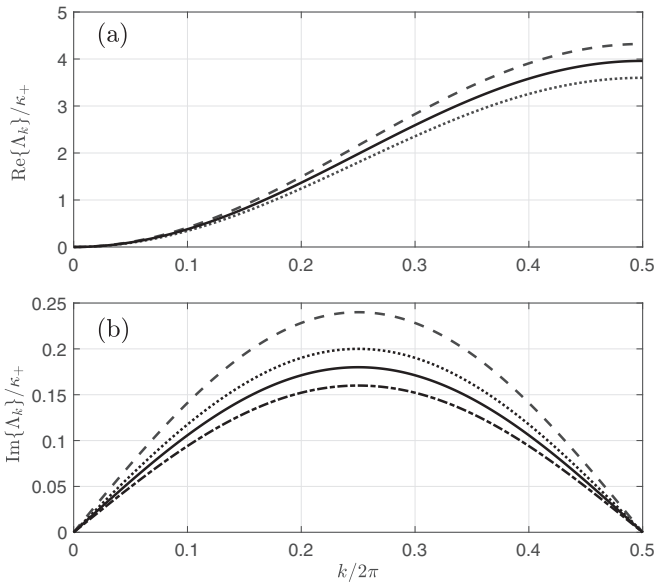

FIG. 7. Real (a) and imaginary (b) parts of the Bogoliubov excitation spectrum. The solid line corresponds to $\rho\alpha = 0.05$, $\rho\beta = 0.1$, the dashed line to $\rho\alpha = 0.1$, $\beta = 0$, the doted line $\alpha = 0$, $\beta = 0$ and the dash-dotted to $\alpha = 0$, $\rho\beta = 0.1$. In all cases $\kappa_-/\kappa_+ = 0.9$.

To calculate the drift thus requires calculation of the expectation values $\langle \hat{c}^\dagger_{k_1}\hat{c}_{k_2}\rangle_{\rm ss}$ and $\langle \hat{c}^\dagger_{k_1}\hat{c}^\dagger_{k_2}\hat{c}_{k_3}\hat{c}_{k_4}\rangle_{\rm ss}$. Writing these expectation values in terms of the $\hat{b}_k$ modes we find

$$\langle \hat{c}^\dagger_{k_1}\hat{c}_{k_2}\rangle_{\rm ss} = \langle Q_0|\hat{b}^\dagger_{k_1}\hat{b}_{k_2}|P(0)\rangle - \frac{\mu_{k_2}}{\Lambda_{k_2}+\Lambda_{-k_2}}\langle Q_0|\hat{b}^\dagger_{k_1}\hat{b}^\dagger_{k_2}|P(0)\rangle \quad (118)$$

$$= N\delta_{k_1,0}\delta_{k_2,0}, \quad (119)$$

as $\mu_0 = 0$. We also find

$$\begin{aligned}\langle \hat{c}^\dagger_{k_1}\hat{c}^\dagger_{k_2}\hat{c}_{k_3}\hat{c}_{k_4}\rangle_{\rm ss} &= \langle Q_0|\hat{b}^\dagger_{k_1}\hat{b}^\dagger_{k_2}\hat{b}_{k_3}\hat{b}_{k_4}|P(0)\rangle \\ &+ \langle Q_0|\hat{b}^\dagger_{k_1}\hat{b}^\dagger_{k_2}\hat{b}_{k_3}\hat{b}^\dagger_{-k_4}|P(0)\rangle\frac{\mu_{k_4}}{\Lambda_{k_4}+\Lambda_{-k_4}} \\ &+ \langle Q_0|\hat{b}^\dagger_{k_1}\hat{b}^\dagger_{k_2}\hat{b}^\dagger_{-k_3}\hat{b}_{k_4}|P(0)\rangle\frac{\mu_{k_3}}{\Lambda_{k_3}+\Lambda_{-k_3}} \\ &+ \langle Q_0|\hat{b}^\dagger_{k_1}\hat{b}^\dagger_{k_2}\hat{b}^\dagger_{-k_3}\hat{b}^\dagger_{-k_4}|P(0)\rangle\frac{\mu_{k_3}\mu_{k_4}}{(\Lambda_{k_3}+\Lambda_{-k_3})(\Lambda_{k_4}+\Lambda_{-k_4})} \quad (120)\end{aligned}$$

$$\begin{aligned}&= \langle Q_0|\hat{b}^\dagger_{k_1}\hat{b}^\dagger_{k_2}\hat{b}_{k_3}\hat{b}_{k_4}|P(0)\rangle \\ &+ \delta_{k_3,-k_4}\langle Q_0|\hat{b}^\dagger_{k_1}\hat{b}^\dagger_{k_2}|P(0)\rangle\frac{\mu_{k_4}}{\Lambda_{k_4}+\Lambda_{-k_4}} \\ &= N^2\delta_{k_1,0}\delta_{k_2,0}\delta_{k_3,0}\delta_{k_4,0} - N\frac{\rho(\alpha+\beta)}{1+2\rho\alpha}\delta_{k_3,-k_4}\delta_{k_1,0}\delta_{k_2,0}, \quad (121)\end{aligned}$$

where in the last line we have used Eqs. (105) and (106) to give

$$\frac{\mu_k}{\Lambda_k+\Lambda_{-k}} = \begin{cases} -\frac{\rho(\alpha+\beta)}{1+2\rho\alpha}, & k\neq 0, \\ 0, & k=0. \end{cases} \quad (122)$$

We arrive at the following result for the drift:

$$v = v_0 + v_0(\alpha-\beta)\left[\rho - \frac{\rho(\alpha+\beta)}{1+2\rho\alpha}\right] \quad (123)$$

$$\approx v_0 + v_0\rho(\alpha-\beta). \quad (124)$$

As we have only expanded the evolution operator to first order in $\alpha\hat{n}_n$ and $\beta\hat{n}_n$, we drop the higher-order terms in Eq. (123) for consistency. Thus, the drift depends on $\alpha-\beta$ and the interactions can increase or decrease the drift depending on the relative magnitudes of α and β. Similar behavior has been identified in Ref. [18,19].

The number fluctuations can also be determined by inserting Eqs. (119) and (121) into Eq. (50):

$$\Delta n = \rho\left[1 - \frac{\rho(\alpha+\beta)}{1+2\rho\alpha}\right] \quad (125)$$

$$\approx \rho[1-\rho(\alpha+\beta)]. \quad (126)$$

Thus, both $\alpha > 0$ and $\beta > 0$ lead to a decrease in onsite number fluctuations.

V. CONCLUSION

In conclusion, using a creation and annihilation operator formalism for indistinguishable classical particles we have derived a master equation for interacting Brownian particles in an out-of-equilibrium periodic potential. This master equation is able to describe regimes spanning the noninteracting to strongly interacting limit.

The discrete master equation is determined from a continuous description of Brownian particles in a deep-well periodic potential by expanding in a set of basis states localized about the minima of each well. In the noninteracting case this reduces to a method developed previously for a single particle [12]. In the interacting case, a self-consistent approach that takes into account the population in each well is required. A particular top-hat interaction potential between particles was assumed. Depending on the width of this potential relative to the width of the wells in the periodic potential, this gives rise to either increased probability of exiting a well or blocking of hopping to neighboring wells.

The master equation resulting from this approach represents a generalization of the well-known ASEP and ZRP. We have shown that it reduces to the ASEP regime in the limit of strong interactions and less than one particle per site, and the ZRP, when the range of the interaction is less then the width of the wells. We have also explored the weak-interaction regime via a Bogoliubov-type approach [21]. In this paper we have focused on calculating the steady-state drift per particle and the number fluctuations. A more comprehensive exploration of this system, including considering more general interaction potentials, is left for future work.

The derivation of the master equation and calculation of observable quantities was greatly facilitated by the use of a creation and annihilation operator description of Brownian particles [13,14]. The operator formalism for Brownian particles, has three key differences to quantum systems:

(1) The evolution operator $\mathcal{L}$ [where $|P(t)\rangle$ is the state of the system and $d|P(t)\rangle/dt = \mathcal{L}|P(t)\rangle$] is nonself adjoint so

left-hand and right-hand basis states are necessary for a full description.

(2) The expectation value of an operator is calculated via $\langle \hat{O} \rangle = \langle Q_0 | \hat{O} | P(t) \rangle$, where $\langle Q_0 | \mathcal{L} = 0$ [see Eq. (8)] rather than $\langle \hat{O} \rangle = \langle P(t) | \hat{O} | P(t) \rangle$ as is usual in quantum mechanics.

(3) Particles satisfy only bosonic statistics.

Despite these differences, many of the well-known properties of the operator formalism still hold and can be used to formulate equations of motion and calculate system averages. More generally, we expect the operator formalism to also be useful for treating interacting Brownian particles in more complicated nonequilibrium systems. For example, the method could be generalized to consider motion in two and three dimensions [33,34], asymmetric interaction potentials [35,36] and even multispecies systems [37].

APPENDIX A: LOCALIZED SINGLE-PARTICLE STATES

Localized single-particle states of a deep-well periodic potential are defined as follows [12]. For the nth potential well of $V_0(x)$ let us denote the minimum as $x = x_n$ and nearest surrounding maxima as $x = b_n$ and $x = a_n$. For each of these wells we can define a metastable potential by

$$\bar{V}_n(x) = \begin{cases} V_0(x) & A_n < x < B_n, \\ -\infty & x = B_n \text{ and } x = A_n, \end{cases} \tag{A1}$$

where the boundaries B_n and A_n of the potential are chosen so that $B_n > b_n$ and $A_n < a_n$. Neighboring metastable potential wells $\bar{V}_{n\pm1}(x)$ overlap in the region around the common maximum $a_n = b_{n-1}$ and $b_n = a_{n+1}$. We can define localized states of the full system in terms of the eigenfunctions of the local metastable potentials as follows:

$$\omega_n^m(x) = \begin{cases} \psi_n^m(x) & A_n \leqslant x \leqslant B_n, \\ 0 & x > B_n \text{ and } x < A_n, \end{cases} \tag{A2}$$

$$\omega_n^{\dagger m}(x) = \begin{cases} \psi_n^{\dagger m}(x) & A_n \leqslant x \leqslant B_n, \\ 0 & x > B_n \text{ and } x < A_n, \end{cases} \tag{A3}$$

where the eigenfunctions $\psi_n^m(x)$ and adjoints $\psi_n^{\dagger m}(x)$ of the nth metastable potential are given by

$$\bar{\mathcal{L}}_n \psi_n^m(x) = -\lambda_n^m \psi_n^m(x), \tag{A4}$$

$$\bar{\mathcal{L}}_n^\dagger \psi_n^{\dagger m}(x) = -\lambda_n^m \psi_n^{\dagger m}(x), \tag{A5}$$

where $\bar{\mathcal{L}}_n$ and $\bar{\mathcal{L}}_n^\dagger$ are, respectively, the evolution operator and its adjoint for the metastable potential $\bar{V}_n(x)$ on the nth well.

In the deep-well limit, the hopping rates Eq. (24) reduce to the well-known Krammer's rates as follows:

$$\kappa_n^+ \approx J(x)\omega_n(x)|_{x=B_n} \tag{A6}$$

$$\approx \frac{[|V''(b_n)|V''(x_n)|]^{\frac{1}{2}}}{2\pi\gamma} e^{-[V_0(b_n)-V_0(x_n)]/k_bT}, \tag{A7}$$

$$\kappa_n^- \approx J(x)\omega_n(x)|_{x=A_n} \tag{A8}$$

$$\approx \frac{[|V''(a_n)|V''(x_n)|]^{\frac{1}{2}}}{2\pi\gamma} e^{-[V_0(a_n)-V_0(x_n)]/k_bT}, \tag{A9}$$

where $V''(y)$ represents the value of the second derivative at position y.

APPENDIX B: ASEP DRIFT AND NUMBER FLUCTUATIONS

In the ASEP only one particle can occupy each site. Each state of the system is therefore a configuration of the N particles across the M sites. The number of possible states is then given by the number of ways of distributing N particles across M sites:

$$\mathcal{N} = \frac{M!}{N!(M-N)!}. \tag{B1}$$

It is convenient to use a binary number decomposition to label each configuration k as

$$k = \sum_{m=1}^{M} B_m^k 2^{M-m}, \tag{B2}$$

where m labels the sites and B_m^k equals 1 (mth site occupied) or 0 (mth site unoccupied). $\sum_{m=1}^{M} B_m^k = N$ ensures conservation of particle number.

In the operator formalism, the configuration k is given by

$$|k\rangle = \prod_{m=1}^{M} \hat{\sigma}_m^{\dagger B_m^k} |\{0\}\rangle. \tag{B3}$$

The steady-state probability is given by the sum over all configurations $|P\rangle_{\rm ss} = \frac{1}{\mathcal{N}} \sum_k^{\mathcal{N}} |k\rangle$. We thus also have $\langle Q_0| = \sum_k^{\mathcal{N}} \langle k|$.

Two key commutator relations allow us to calculate the averages in the steady state:

$$\left[\hat{\sigma}_n, \prod_{m=1}^{M} \hat{\sigma}_m^{\dagger B_m^k}\right] = \begin{cases} B_n^k \prod\limits_{\substack{m=1 \\ m\neq n}}^{M} \hat{\sigma}_m^{\dagger B_m^k} & \text{if } n \leqslant M, \\ 0 & \text{if } n > M, \end{cases} \tag{B4}$$

$$\left[\prod_{m'=1}^{M} \hat{\sigma}_{m'}^{B_{m'}^{k'}}, \hat{\sigma}_n^\dagger\right] = \begin{cases} B_n^{k'} \prod\limits_{\substack{m'=1 \\ m'\neq n}}^{M} \hat{\sigma}_{m'}^{B_{m'}^{k'}} & \text{if } n \leqslant M, \\ 0 & \text{if } n > M. \end{cases} \tag{B5}$$

We illustrate this by calculating the $\langle \hat{\sigma}_{n+1}^\dagger \hat{\sigma}_n \rangle_{\rm ss}$:

$$\langle \hat{\sigma}_{n+1}^\dagger \hat{\sigma}_n \rangle_{\rm ss} \tag{B6}$$

$$= \frac{1}{\mathcal{N}} \sum_{k,k'=1}^{\mathcal{N}} \left\langle \{0\} \middle| \prod_{m'=1}^{M} \hat{\sigma}_{m'}^{B_{m'}^{k'}} \hat{\sigma}_{n+1}^\dagger \hat{\sigma}_n \prod_{m=1}^{M} \hat{\sigma}_m^{\dagger B_m^k} \middle| \{0\} \right\rangle \tag{B7}$$

$$= \frac{1}{\mathcal{N}} \sum_{k,k'=1}^{\mathcal{N}} B_{n+1}^{k'} B_n^k \left\langle \{0\} \middle| \prod_{\substack{m'=1 \\ m'\neq n+1}}^{M} \hat{\sigma}_{m'}^{B_{m'}^{k'}} \prod_{\substack{m=1 \\ m\neq n}}^{M} \hat{\sigma}_m^{\dagger B_m^k} \middle| \{0\} \right\rangle, \tag{B8}$$

where in the second line we have used the commutation relations Eq. (B4) and (B5). For the sum on the right-hand side to be nonzero, we require that $B_{n+1}^{k'} = 1$, $B_n^k = 1$ and

$$B_m^k = B_m^{k'} \qquad (m \neq n, m \neq n+1), \tag{B9}$$

$$B_{n+1}^k = 0, \qquad B_n^{k'} = 0. \tag{B10}$$

Using Eq. (B2) and these restrictions on the binary coefficients, we can write k' in terms of k in the second sum. Specifically, we require that the configuration k' has the site n unoccupied and site $n+1$ occupied and the rest of the

configuration is identical to k. With this restriction we can now write

$$\langle \hat{\sigma}_{n+1}^{\dagger} \hat{\sigma}_n \rangle_{\rm ss} = \frac{1}{\mathcal{N}} \sum_{k=1}^{\mathcal{N}} \left(B_n^k - B_n^k B_{n+1}^k \right). \tag{B11}$$

The first term represents all the configurations which have site n occupied and the second the number of configurations where both n and $n+1$ are occupied. The number of configurations with two sites occupied is the number of ways of arranging $N-2$ particles in $M-2$ sites. This gives the solution in terms of binomial coefficients

$$\langle \hat{\sigma}_{n+1}^{\dagger} \hat{\sigma}_n \rangle = \binom{M}{N}^{-1} \left[\binom{M-1}{N-1} - \binom{M-2}{N-2} \right] \tag{B12}$$

$$= \binom{M}{N}^{-1} \binom{M-2}{N-1} \tag{B13}$$

$$= \frac{N(M-N)}{M(M-1)}. \tag{B14}$$

A similar calculation gives

$$\langle \hat{\sigma}_n^{\dagger} \hat{\sigma}_n \rangle_{\rm ss} = \frac{1}{\mathcal{N}} \sum_{k=1}^{\mathcal{N}} B_n^k \tag{B15}$$

$$= \frac{1}{\mathcal{N}} \binom{M-1}{N-1} \tag{B16}$$

$$= \frac{N}{M}, \tag{B17}$$

where in the second line we have used the fact that $\sum_{k=1}^{\mathcal{N}} B_n^k$ is the number of configurations with site n occupied, i.e., there are $N-1$ particles left to arrange in $M-1$ sites.

[1] M. Evstigneev, S. von Gehlen, and P. Reimann, Phys. Rev. E **79**, 011116 (2009).
[2] C. T. MacDonald, J. H. Gibbs, and A. C. Pipkin, Biopolymers **6**, 1 (1968).
[3] D. Chowdhury, Phys. Rep. **529**, 1 (2013).
[4] E. Frey and K. Kroy, Ann. Phys. **14**, 20 (2005).
[5] C. Lutz, M. Kollmann, and C. Bechinger, Phys. Rev. Lett. **93**, 026001 (2004).
[6] F. Evers, R. D. L. Hanes, and C. Zunke *et al.*, Eur. Phys. J. Spec. Top. **222**, 2995 (2013).
[7] K. Nelissen, V. R. Misko, and F. M. Peeters, Europhys. Lett. **80**, 56004 (2007).
[8] A. Taloni and F. Marchesoni, Phys. Rev. Lett. **96**, 020601 (2006).
[9] T. Chou, T. K. Mallick, and R. K. P. Zia, Rep. Prog. Phys. **74**, 116601 (2011).
[10] P. Reimann, Phys. Rep. **361**, 57 (2002).
[11] K. J. Challis and M. W. Jack, Phys. Rev. E **88**, 042114 (2013).
[12] P. T. T. Nguyen, K. J. Challis, and M. W. Jack, Phys. Rev. E **94**, 052127 (2016).
[13] M. Doi, J. Phys. A: Math. Gen. **9**, 1465 (1976).
[14] M. Doi, J. Phys. A: Math. Gen. **9**, 1479 (1976).
[15] F. Spitzer, Adv. Math. **5**, 246 (1970).
[16] M. R. Evans and T. Hanney, J. Phys. A: Math. Gen. **38**, R195 (2005).
[17] M. R. Evans and B. Waclaw, J. Phys. A: Math. Theor. **47**, 095001 (2014).
[18] D. Lips, A. Ryabov, and P. Maass, Phys. Rev. Lett. **121**, 160601 (2018).
[19] D. Lips, A. Ryabov, and P. Maass, Phys. Rev. E **100**, 052121 (2019).
[20] D. C. Mattis and M. L. Glasser, Rev. Mod. Phys. **70**, 979 (1998).
[21] A. L. Fetter and J. D. Walecka, *Quantum Theory of Many-particle Systems* (Dover, Mineola, NY, 2003).
[22] G. M. Schütz, The space-time structure of extreme current and activity events in the ASEP, in *Nonlinear Mathematical Physics and Natural Hazards* (Springer, Cham, 2015), pp. 13–28.
[23] F. van Wijland and Z. Rácz, J. Stat. Phys. **118**, 27 (2005).
[24] C. W. Gardiner, *Handbook of Stochastic Methods for Physics, Chemistry, and the Natural Sciences*, 4th ed. (Springer, Berlin, 2009).
[25] H. Risken, *Fokker-Planck Equation* (Springer, Berlin, 1996).
[26] M. O. Magnasco, Phys. Rev. Lett. **72**, 2656 (1994).
[27] D. Keller and C. Bustamante, Biophys. J. **78**, 541 (2000).
[28] C. W. Gardiner and P. Zoller*Quantum Noise: A Handbook of Markovian and Non-Markovian Quantum Stochastic Methods with Applications to Quantum Optics*, 3rd ed. (Springer-Verlag, New York, NY, 2004).
[29] F. H. Essler, V. and Rittenberg, J. Phys. A: Math. Gen. **29**, 3375 (1996).
[30] L. H. Gwa and H. Spohn, Phys. Rev. Lett. **68**, 725 (1992).
[31] D. Kim, Phys. Rev. E **52**, 3512 (1995).
[32] L. Pitaevskii and S. Stringari, *Bose-Einstein Condensation* (Clarendon Press, Oxford, UK, 2003).
[33] T. Vicsek, A. Czirok, E. Ben-Jacob, I. Cohen, and O. Shochet, Phys. Rev. Lett. **75**, 1226 (1995).
[34] M. C. Marchetti, J. F. Joanny, S. Ramaswamy, T. B. Liverpool, J. Prost, M. Rao, and R. A. Simha, Rev. Mod. Phys. **85**, 1143 (2013).
[35] A. Doostmohammadi, J. Ignés-Mullol, J. M. Yeomans and F. Sagués, Nat. Commun. **9**, 3246 (2018).
[36] R. Großmann, I. S. Aranson, and F. Peruani, Nat. Commun. **11**, 5365 (2020).
[37] S. C. Takatori and J. F. Brady, Soft Matter **11**, 7920 (2015).